An evaluation method for displacement-dependent slope stability

Shiguo Xiao[1,2]

[1] Key Laboratory of High-speed Railway Engineering, Ministry of Education, Southwest Jiaotong University, Chengdu 610031, China.
[2] Department of Geological Engineering, Southwest Jiaotong University, Chengdu 610031, China.

ABSTRACT

For a sliding slope, its stability is greatly influenced by its displacements. Based on the definition of coefficient of slope stability from deformation energy, an analysis procedure of displacement-dependent stability of slope is proposed using numerical simulation method with shear strength reduction. This new method removes limitations seen in those without establishing the rational relationship between slope stability with its displacements. Variation of deformation parameters of slope are significantly involved in the process of shear strength reduction via numerical simulation. So the coefficient of slope stability is coupled with the slope displacements by the shear strength reduction with the newly altered deformation parameters. Two typical slope examples are analyzed to show the easy utilization of the proposed method in numerical simulation. The results indicate an exponential decrease in the coefficient of stability with the slope displacements in increase. The displacement-dependent coefficient of stability provides base for quantitatively gaining slope stability through monitoring the slope displacements.

Keywords: slope stability; deformation energy; coefficient of stability; displacement; shear strength reduction

1 INTRODUCTION

The calculation methods of slope stability (Bishop 1955; Morgenstern and Price 1965; Spencer 1967; Sarma 1979) are largely developed in light of limit equilibrium method (LEM). They are convenient to being used to obtain factor of safety (or coefficient of stability) of a slope. However, they have disadvantages in analyzing the stress field and displacement field of a slope which can be easily gained by numerical simulation method (NSM) (Duncan 1996). The simulation method for stability analysis of a slope is generally conducted through strength reduction technique (Zienkiewicz et al. 1975; Dawson and Roth 1999; Isakov and Moryachkov, 2014), despite the controversies about slope destabilization criteria (Cala et al. 2004). Factor of safety may be estimated using (1) force balance, after stress on a slip surface is estimated complicatedly through interpolation of numerical results (Zou et al. 1995); (2) finite element arc search method (Kalatehjari et al. 2014) for an arc shape slip surface in spite of the practical slip surface being not circular arc; and be estimated as (3) the ratio of the sum of limit resistances along slip surface over that of actual shear forces (e.g. Krahn 2003), although it cannot be simply done through superposition, due to different action directions of tangential shear resistances or stresses on various sections along non-linear slip surface. However, slope stability is practically linked closely with displacement of slope, which is not reflected correctly in all above-mentioned factor of safety. Especially for the shear strength reduction method (SSRM), slope displacement is gradually growing in the process of reduction coefficient of shear strength being increased. It means actually that the higher factor of safety is, the higher displacement of a slope is, which is contradictory to engineering practice.

As for study of energy method involved in slope displacement for stability analysis of a slope, Ekanayake and Phillips (1999) discussed subsurface stability of vegetated hillslopes by an energy method using measured shear stress and displacement curve. The method may be applicable to a shallow sliding but not for a deep sliding slope. The measured shear displacement is a tangent displacement along the slip surface, and is less visual and inconvenient to be detected on the slope free surface.

In view of the limitations for each method mentioned above, a novel factor of safety was proposed on the basis of deformation and potential energy (Xiao et al. 2018). The concept of factor of safety can be used in both LEM and NSM. According to the definition on factor of safety of slope stability, a new analysis method carried out via numerical simulation for displacement-dependent slope stability is elaborated herein, and two examples including a monitored slope is applied to predict its coefficient of stability.

2 COEFFICIENT OF SLOPE STABILITY

Deformation energy increases in a material with loading until it reaches an upper limit, and the material fails. So, coefficient of stability of a slope (along a slip surface) is defined as the root of the ratio of ultimate deformation energy (e_u) over the accumulated (elastic) deformation energy (e_a) corresponding to actual deformation (Xiao et al. 2018). Based on principles of energy conservation, the deformation energy along a slip surface must be equal to the gravitation potential energy of the corresponding (rigid) slide mass bounded by the slip surface and the free surface (see Fig. 1(a)). Then, the coefficient of stability K_s of the slide mass along the slip surface is expressed as:

$$K_s = \sqrt{e_u / e_a} \tag{1}$$

where e_u and e_a are the limit and 'elastic' (gravitation) potential energy of a slide mass, respectively.

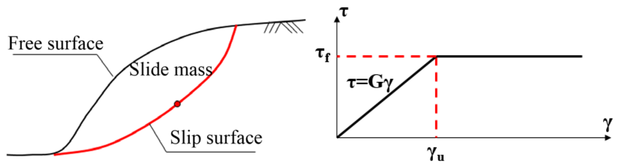

(a) (b)
Fig. 1. A slope with potential slip surface (a) slide mass; (b) Elastic-perfectly plastic τ-γ curve.

3 DISPLACEMENT VERSUS COEFFICIENT OF STABILITY

Since gravitation potential energy of a potential slide mass is equal to gravity multiplied by vertical displacement of centroid of the mass, it can be figured out if the shape of slide mass under various conditions of developed shear strength of slip surface of the slope is determined. By using shear strength reduction technology of sliding zone of a slope in NSM with a reduction factor and four new deformation parameters (proposed here), the problem can be solved.

The calculation procedure, as outlined next, includes determination of critical slip surface, potential energy e_u and e_a, displacements of slide mass for typical reduction factors, and related coefficients of stability.

First, numerical simulation model is set up for a slope to obtain the critical slip surface and corresponding slide mass using SSRM. The shape of the slide mass can be obtained easily by **Phase²** program (Rocscience Inc., 2014). The related reduction factor ψ_u in the ultimate state is simultaneously gained.

Second, the modified deformation and shear strength parameters are obtained to compute ultimate (gravitation) potential energy e_u in the same numerical simulation model. With the elastic-perfectly plastic shear stress $\tau \sim$ shear strain γ curve (see Fig. 1(b)) at any point on a potential slip surface, the ultimate state occurs at a shear strain $\gamma_u = \tau_f/G_0$, where τ_f is shear stress in the limit state. Using strength reduction with factor ψ_u in the ultimate state leads to $\gamma_u = (\tau_f/\psi_u)/G_u$, and furthermore modulus reduction of $G_u = G_0/\psi_u$, in which G_u and G_0 are shear modulus in the ultimate state (after shear strength reduction) and initial condition, respectively. Based on stress state of a point in semi-infinite elastic body and Mohr-Coulomb failure criterion (Zheng et al., 2005), a calculation parameter β no less than 1 can be expressed as:

$$\beta = \sin\phi / (1 - 2\mu) \tag{2}$$

where, ϕ is the internal friction angle and μ is Poisson's ratio of soil. The parameter β maintains as a constant without any reduction (Zheng et al. 2005), which has limited impact on the solution of slope stability.

According to Eq. (2) and considering Young's modulus E [$= 2(1+\mu)G$], elastic deformation parameters of the slope can be deduced as:

$$\frac{\mu}{\mu_u} = \frac{1 - \sin\phi/\beta}{1 - \sin[\arctan(\tan\phi/\psi)]/\beta} \tag{3}$$

$$\frac{E}{E_u} = \frac{(3 - \sin\phi/\beta)\psi}{3 - \sin[\arctan(\tan\phi/\psi)]/\beta} \tag{4}$$

Additionally, shear strength parameters can be generally expressed as (Zienkiewicz et al. 1975):

$$c/c_u = \psi \tag{5}$$

$$\tan\phi/\tan\phi_u = \psi \tag{6}$$

where c_u, ϕ_u, μ_u and E_u are cohesion, angle of internal friction, Poisson's ratio, and elastic modulus in the ultimate state, respectively. For the critical slide mass obtained in the ultimate state using the modified values of c_u, ϕ_u, E_u and μ_u in NSM, limit (gravitation) potential energy e_u in Eq. (1) is determined via its self-weight multiplied by vertical displacement of its centroid relative to the initial condition based on its coordinates.

Third, with the reduction factor in limit state ψ_u obtained, a series of new reduction factor of shear strength ψ_i ($1 \le \psi_i \le \psi_u$) for elastic state are selected as $\psi_i = 1 + (\psi_u - 1)i/n$ and i = 1, 2, …, n-1 (n is total selected numbers of reduction factors and $n \ge 10$ is suggested to ensure accuracy) to obtain elastic displacement of the slope prior to limit state. The detailed procedures are as follows:

- The strength parameter c_i and ϕ_i, and deformation parameter μ_i (≤ 0.5) and E_i for a selected ψ_i are estimated by using Eqs. (3) to (6) in which the subscript 'u' is replaced with subscript 'i'.
- Displacement field of the slope for ψ_i is obtained using NSM with the corresponding four parameters. This yields a new sliding shape and its centroid coordinates x_c and y_c (for the **same** slide mass and boundary in critical state), and allows the gravitation potential energy e_a and the coefficient of stability (using Eq. (1)) to be estimated.
- Repeating the calculation for a series of ψ_i gains the relationship between K_s and displacement (including horizontal, vertical or total movement) of any point on the slope face or in the slide mass.

4 EXAMPLES

The proposed method is adopted to study stability of a soil slope with uniform properties (Hassiotis et al. 1997). The slope has dimensions (in m) and material parameters shown in Fig. 2(a), including unit weight γ, cohesion c, angle of internal friction ϕ, Poisson's ratio μ, and elastic modulus E, respectively. The load considered is only the self-weight of soil slope.

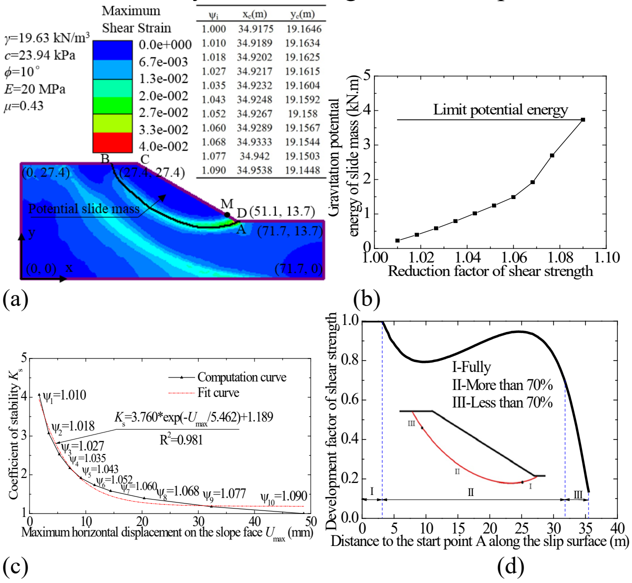

Fig. 2. Simulation of a slope by FEM using SSRM: (a) Slide mass obtained; (b) Potential energy versus reduction factor (c) Slope displacement versus stability coefficient; (d) Non-uniform mobilization of shear strength along critical slip surface.

The example is analyzed using the finite-element method (FEM) via **Phase²** program (Rocscience Inc., 2014). For simplicity, the slope material is stipulated as elastoplastic material obeying a non-associative plastic flow rule (dilation angle = 0) and Mohr-Coulomb's failure criterion. The FEM adopts 6-noded triangular elements. The numerical analysis offers the stress field of the slope, and the slip surface in critical state.

The evolution of coefficient of stability K_s with displacement is calculated for the uniform slope. The FEM simulation using ψ_u =1.09 offers a slide mass ABCD with area 188.51m^2 (see Fig. 2(a)), and the centroid co-ordinates x_c (horizontal) and y_c (vertical) in elastic (for different ψ_i) and critical state (for ψ_u). The gravitation potential energy of the slide mass e_a is thus calculated (see Fig. 2(b)). Fig. 2(c) shows the exponential reduction of K_s with the maximum horizontal displacement U_{max} at the point of maximum horizontal movement along the slope face M (ψ_u =1.09, see Fig. 2(a)) on the slope free surface. The K_s is infinite large at zero slope displacement (due to zero deformation energy e_a), and reduces to 1.0 (limit state) at a displacement of 48.75 mm. The shear strength is mobilized to different degree (τ_i/τ_{fi}) along the slip surface (see Fig. 2(d)). The shear stress attains the limit τ_{fi} near the slope toe (i.e. I region), over 70% the limit τ_{fi} in the middle (II) region, and less than 70% close to the crest (III region), respectively. As shown in Fig. 3, if the traditional shear strength reduction method is carried out via numerical simulation, the coefficient of slope stability is increasing as the slope displacement increases. This is undoubtedly irrational.

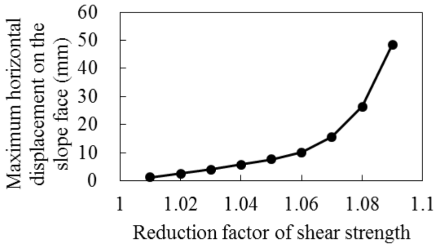

Fig. 3. Relationship between the slope displacements with its coefficient of stability obtained using traditional shear strength reduction in numerical simulation method.

Under the condition that dilation angle of soil is equal to zero, the sensitivity of the coefficient of stability K_s at a measured displacement U_{max} to the input parameters c, ϕ, E, and μ was examined. The K_s versus U_{max} curves are plotted in Fig. 4, respectively. The coefficient of stability K_s increases with increase in shear strength (via c, ϕ) at a given U_{max}, but decreases with E increase. This trend is reasonable. The impact of Poissons' ratio μ on the factor K_s is negligibly small.

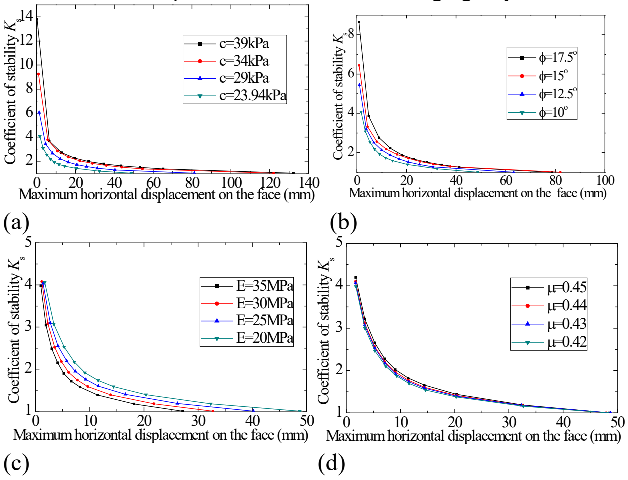

Fig. 4. K_s-U_{max} curves to soil properties: (a) c; (b) ϕ; (c) E; (d) μ.

Additionally, the reduction of factor of safety with slope movement is also useful to determine K_s for a measured nonhomogeneous slope displacement. It can reflect evolution of local stability of the slope area near the monitored points. A colluvial landslide No.1 Wan-zhou-tang-jiao in the Three Gorges Reservoir, as shown in Fig. 5(a) (Tang 2013), is studied here as an example. The soil properties are given in Table 1. Horizontal displacements of the points WZ13-07 and WZ13-08 on the free surface (see Fig. 5(a)) were monitored and are shown in Fig. 5(b). The current method estimates a coefficient of stability of the slope K_s of 1.19 on 1 September 2009 for point WZ13-07 at a monitored horizontal displacement of 70 mm; and a coefficient of stability K_s of 1.58 for point WZ13-08 at a displacement of 140 mm (see Fig. 5(c)), respectively. Because the ultimate displacement at point WZ13-07 and WZ13-08 are about 100mm and 400mm (see Fig. 5(c)), respectively, the ratio of the ultimate displacement at point WZ13-07 over its actual displacement on 1 September 2009 is less than that at point WZ13-08. Thus, the K_s at point WZ13-08 is more than that at point WZ13-07. But they are both more than 1. As a matter of fact, the area of the slope in which the two monitored points are located is in stable state (Tang 2013), so the presented method for quantitatively predicting local or overall stability of a monitored slope is applicable.

5 CONCLUDING REMARKS

A method is proposed for assessing slope stability related to the slope displacements based on the definition of coefficient of stability from deformation energy. It is easy to handle in NSM with varied deformation parameters of the slope in the process of shear strength reduction. The coefficient of stability can be reasonably coupled with the slope displacements, which cannot be properly reflected in the traditional NSM with shear strength reduction. The displacement-dependent coefficient of stability reduces as the slope displacement increases, and allows factor of safety of the slope to be calculated for each monitored slope displacement.

ACKNOWLEDGEMENTS

The research was supported by Chinese National Natural Science Foundation (Grant No. 51578466).

REFERENCES

Bishop, A. W. (1955). The use of the slip circle in the stability analysis of slopes. Geotechnique, 5(1), 7-17.
Cala, M., Flisiak, J., and Tajdus, A. (2004). Slope stability analysis with modified shear strength reduction technique. In Proceedings of the Ninth International Symposium on Landslides'04, RiodeJanerio. London: A.A. Balkema Publishers, pp 1085-1089.
Dawson, E. M. and Roth, W. H. (1999). Slope stability analysis by strength reduction. Geotechnique, 49(6), 835-840.
Duncan, J. M. (1996). State of the art: limit equilibrium and finite element analysis of slopes. Journal of Geotechnical Engineering, 122(7), 577-596.
Ekanayake, J. C. and Phillips, C. J. (1999). A method for stability analysis of vegetated hillslopes: an energy approach.
Hassiotis, S., Chmaeau, J. L., and Gunarante, M. (1997). Design method for stabilization of slopes with piles. Journal of Geotechnical and Geoenvironmental Engineering, 123(4), 314-323.
Isakov, A. and Moryachkov, Y. (2014). Estimation of Slope Stability Using Two-Parameter Criterion of Stability. International Journal of Geomechanics, 14(3), 06014004.
Kalatehjari, R., Ali, N., Kholghifard, M., and Hajihassani, M. (2014). The effects of method of generating circular slip surfaces on determining the critical slip surface by particle swarm optimization. Arabian Journal of Geosciences, 7(4), 1529-1539.
Krahn, J. (2003). The 2001 R.M. Hardy Lecture: The limits of limit equilibrium analyses. Canadian Geotechnical Journal, 40(3), 643-660.
Morgenstern, N. R. and Price, V. (1965). The analysis of the stability of general slip surface. Geotechnique, l5(1), 79-93.
Sarma, K. S. (1979). Stability analysis of embankments and slopes. Journal of Geotechnical Engineering, ASCE, 105(12), 1511-1524.
Spencer, E. (1967). A method of analysis of embankments assuming parallel inter-slice forces. Geotechnique, 17(1), 11-26.
Tang, L. (2013). Research on Stability and Prediction for the colluvial landslide in the Three Gorges Reservoir. Dissertation, China University of Geosciences at Wuhan.
Rocscience Inc. Shear Strength Reduction Analysis. Available from: <https: //www. rocscience. com/ help/ phase2/ webhelp/ tutorials/ Phase2_Tutorials.htm>. [20 November 2014].
Xiao, S. G., Guo, W. D., and Zeng, J. X. (2018). Factor of safety of slope stability from deformation energy. Canadian Geotechnical Journal, 55(2), 296-302.
Zheng, H., Liu, D. F. and Li, C. G. (2005). Slope stability analysis based on elasto-plastic finite element method. International Journal for Numerical Methods in Engineering, 64(14), 1871-1888.
Zienkiewicz, O. C., Humpheson, C. and Lewis, R. W. (1975). Associated and non-associated visco-plasticity and plasticity in soil mechanics. Geotechnique, 25(4), 671-689.
Zou, J. Z., Williams, D. J., and Xiong, W. L. (1995). Search for critical slip surface based on finite element method. Canadian Geotechnical Journal, 32(2), 233-246.

Table 1. Soil properties of landslide No. 1 in the Three Georges Reservoir (Tang, 2013)

Stratum	Unit weight (kN/m^3)	Cohesion (kPa)	Angle of internal friction (degrees)	Elastic modulus (MPa)	Poisson's ratio
Potential slide mass	20.7	20.4	13.50	36.5	0.39
Slip band with thickness 2m	20.0	16.9	11.81	30.0	0.40
Stable layer	25.0	228.0	34.20	2000.0	0.25

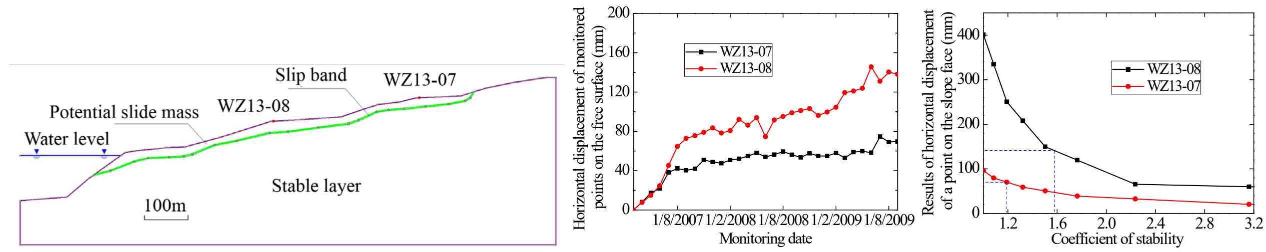

(a) (b) (c)

Fig. 5. Landslide No.1 Wan-zhou-tang-jiao in the Three Gorges Reservoir: (a) Sketch of the landslide, (b) Measured horizontal displacement at two points on the free face; (c) Horizontal displacement versus coefficient of stability of the slope